

Polyaniline as a dual flame retardant and electrostatic dissipative additive in polyethylene nanocomposites

Akeem Adisa¹ | Joseph K. O. Asante² | Vincent O. Ojijo³ |
 António B. Mapossa⁴ | Washington Mhike¹ 

¹Polymer Technology Division,
 Department of Chemical, Metallurgical
 and Materials Engineering, Tshwane
 University of Technology, Pretoria,
 South Africa

²Department of Physics, Tshwane
 University of Technology, Pretoria,
 South Africa

³Centre for Nanostructures and Advanced
 Materials, DSI-CSIR Nanotechnology
 Innovation Centre, Council for Scientific
 and Industrial Research, Pretoria,
 South Africa

⁴Department of Chemical and Petroleum
 Engineering, University of Calgary,
 Calgary, Alberta, Canada

Correspondence

Washington Mhike, Polymer Technology
 Division, Department of Chemical,
 Metallurgical and Materials Engineering,
 Tshwane University of Technology,
 Pretoria 0183, South Africa.
 Email: mhikew@tut.ac.za

Funding information

Tshwane University of Technology

Abstract

Polyolefins, such as polyethylene (PE), are highly flammable and electrically insulative, limiting their applicability. The study explored the flame-retardancy and electrical conductivity of PE/polyaniline (PE/PANI) nanocomposites containing undoped PANI, PANI doped, and co-doped with various acids and PANI modified with a double layered hydroxide or ammonium polyphosphate (APP). The nanocomposites were synthesized through in situ chemical oxidative polymerization of aniline and compression molding. Flame retardancy was evaluated using UL 94 tests and cone calorimetry. All nanocomposites, except the de-doped PANI nanocomposite, attained a UL 94 V2 rating. Cone calorimeter results showed that PANI doped with H₃PO₄ reduced the peak heat release rate by 20% compared to neat PE, whereas co-doping PANI with H₃PO₄ and phytic acid reduced it by 31%. The nanocomposites exhibited volume resistivity for suitable for electrostatic dissipation applications but showed marginally reduced mechanical properties. This study demonstrates the potential to develop electrostatic dissipative and flame-retardant PE nanocomposites incorporating PANI.

Highlights

- PE/PANI nanocomposites were synthesized.
- PANI doped with H₃PO₄ reduced the peak HRR by 20%.
- Co-doping PANI with H₃PO₄ and phytic acid further reduced peak HRR.
- Nanocomposites attained a UL 94 V2 rating.
- PE/PANI nanocomposites were electrostatic dissipative.

KEYWORDS

dopants, electrostatic dissipation, flame retardant, polyaniline, polyethylene

1 | INTRODUCTION

Polyethylene (PE) is the most widely used commodity polymer due its desirable properties, such as ease of processability, low cost, flexibility, toughness at

ambient temperatures, good chemical resistance, and non-toxicity.^{1,2} However, similar to other polyolefins, PE is a hydrocarbon that lacks charge carriers such as ions or free electrons, which restricts their mobility.³

This is an open access article under the terms of the [Creative Commons Attribution](https://creativecommons.org/licenses/by/4.0/) License, which permits use, distribution and reproduction in any medium, provided the original work is properly cited.

© 2024 The Author(s). Journal of Vinyl & Additive Technology published by Wiley Periodicals LLC on behalf of Society of Plastics Engineers.

Consequently, polyolefins including PE, are highly flammable and non-electrically conductive, with volume resistivity values that range from 10^{15} to 10^{22} Ω cm.⁴ PE has a low limiting oxygen index (LOI), a high heat of combustion and high a heat release rate (HRR), which contributes to its tendency to burn easily, drip while burning and leave no residual char. It thus leads to rapid flame spread.^{1,2}

The high flammability and low electrical conductivity of PE limits its applications. For instance, underground mining applications such as sheathing, piping, and casings require plastics materials with low flammability to reduce fire hazards and electrical conductivity to prevent static charge build-up. Static charges can be incendiary by being ignition sources and causing explosions or fires. To meet stringent fire safety standards, PE used in these applications is often incorporated with flame-retardant additives and antistatic agents.¹

A variety of flame retardants have been developed to enhance the flame-retardant performance of polyethylene. Despite their effectiveness, halogenated flame retardants are no longer widely used due to their tendency to corrode processing equipment, and emit toxic gases during fires as well as environmental concerns. Consequently, there has been a shift towards halogen free flame retardants such as metal hydroxides, phosphorus, and nitrogen-based flame retardants and intumescent flame retardants (IFRs).^{1,2,5}

However, the aforementioned flame retardants have significant limitations when used in PE. For example, metal hydroxides, such as magnesium and aluminium hydroxide, impart flame retardancy in PE at high contents (> 40 wt.%). This leads to deterioration in mechanical, physical, and rheological properties, as well as the processability of the PE.^{1,2,6} Phosphorus-based flame retardants include red phosphorus, phosphines, phosphine oxides, phosphonium compounds, phosphonates, phosphites, phosphinates, and phosphates.⁶ While effective, phosphorus-based flame retardants easily absorb water, generate excessive amounts of smoke and volatiles during processing, limiting their applications. Despite these drawbacks, phosphorus-based flame retardants are often combined other flame retardants, to achieve a synergistic effect.²

Nitrogen-based flame retardants can function in the vapor phase by releasing non-flammable gases such as NH_3 and N_2 , which dilute the combustion process.⁷ While they are less effective than halogen-based flame retardants, they are relatively non-toxic, produce low smoke emissions during fires and they are environmentally friendly. Common nitrogen-based flame retardants include melamine, triazine, urea (phosphate), and guanidine based compounds.⁶ Additionally, nitrogen-based

flame retardants can synergistically enhance the flame retardancy of phosphorus-based flame retardants.^{7,8}

IFRs swell when exposed to fire or heat, forming a carbonaceous, porous char that acts as a barrier to heat, oxygen and the other pyrolysis products.⁶ IFRs primarily function through a condensed phase mechanism to impart flame retardancy. IFRs consist of an acid, a carbonizing or char foaming agent and a foaming agent. Their advantages include high flame-resistance efficiency, anti-dripping properties, non-toxicity, and environmental friendliness. IFRs are among the most effective flame retardants for PE.² However, recent studies on IFRs have focused on addressing their exudation and water solubility challenges, as well as enhancing the mechanical properties of polymers incorporated with IFRs.⁶

Due to growing environmental and health concerns, there is a push for safer and greener flame retardants. Stricter regulations are also driving these efforts. As a result, more research is focused on developing flame retardants that are less harmful to people and the environment.⁷

Polyaniline (PANI) is a widely studied intrinsically conducting polymer due to its relatively low cost, ease of synthesis, good chemical stability, good processability, and tuneable electrical conductivity. Its conductivity arises from the conjugated π -electron system in its structure.⁹ Depending on its oxidation state, PANI contains nitrogen in the form of amines or imines sandwiched in-between benzenoid and quinoid rings.

PANI exhibits two major limitations; it cannot be processed by conventional polymer melting processing techniques such as extrusion, and it exhibits poor mechanical properties. Consequently, PANI is often blended with other polymers to fabricate conductive blends and composites.¹⁰⁻¹² However, there have been limited studies on the flame retardancy of PANI.^{7,13}

Zarrintaj et al.⁷ suggested that PANI, due to its nitrogen content, has the potential to be an effective flame retardant with electroactive properties. They emphasized that careful selection of a dopant for PANI was necessary in utilizing it as a flame retardant. The thermal degradation of PANI could produce gaseous products such as CO_x , NO_x , and H_2O , together with vaporized dopant molecules or degraded products and dopants. Additionally, PANI could act as a potential char precursor.⁷ However, there have been a few studies in which PANI was utilized as a flame retardant for polymers.

For instance, Bhat et al.¹⁴ observed that PANI coated cotton fabrics had improved ignition resistance compared to neat cotton. Stejskal et al.¹⁵ found that cellulose fibers coated with PANI produced solid carbonaceous by-products that functioned as a barrier to oxygen,

enhancing the flame retardancy of the cellulose fibers. Salgaonkar and Jayaram¹⁶ studied polyester fabric grafted with PANI and observed that the PANI increased the LOI of the fabrics and produced a high char yield. Zhang et al.¹⁷ fabricated electrically conductive and flame-retardant epoxy/PANI nanocomposites. They found that the PANI reduced the HRR of the epoxy and also enhanced char formation. In this study it was also observed that the PANI nanofibre particles produced lower peak heat release rates (pHRRs) compared to the PANI nanospherical particles. This was attributed to the higher surface areas of the PANI nanofibres.

In the few studies that have been conducted with PANI as a flame retardant, the choice of dopant had a significant effect. This was apparent in the study by Wu et al.¹³ in which they investigated the flame retardancy and conductivity of PANI-deposited paper composites doped with phosphoric acid (H_3PO_4), hydrochloric acid (HCl), and sulfuric acid (H_2SO_4). They found that H_3PO_4 was the best dopant with respect to enhancing flame retardancy in terms of the LOI values, whereas H_2SO_4 imparted the best conductivity values. However, the study also showed that co-doping of the PANI with equimolar mixtures of either H_3PO_4 and H_2SO_4 or H_3PO_4 and HCl produced optimum enhanced conductivity and flame-retardant properties of the composite. Yu et al.⁸ also obtained excellent flame retardancy with respect to combustion ratios and LOI values of polyester fabrics coated with in situ polymerized polyaniline co-doped with HCl and H_3PO_4 . The modified polyester fabrics also exhibited excellent electrical conductivity of up to 17.8 S/cm. The study by Yu et al.⁸ revealed that the oxidant (ammonium persulfate)/aniline ratio had an effect on both the flame retardancy and electrical conductivity. Mao et al.¹⁸ utilized p-toluene sulfonic acid (PTSA) and sulfosalicylic acid (SSA) as dopants, in preparing polyaniline-deposited functional cellulosic paper. The SSA doped polyaniline-deposited functional cellulosic paper had better conductivity and LOI values, compared to the PTSA doped one.

Recently, several studies have focused on using PANI as a flame retardant for epoxy resins (EPs). For example, Zhong et al.,¹⁹ enhanced PANI's flame retardancy by doping it with phytic acid and copper ions, forming a dendritic structure that improved dispersion and resulted in an epoxy composite coating with superior fire resistance, lower smoke density, and high carbon residue. Chen et al.,²⁰ demonstrated that PANI-graphitized carbon nitride nanosheets doped amino trimethyl phosphonic acid provided better flame retardancy, while those doped with phytic acid significantly enhanced fire safety when used as a synergist for IFRs. Additionally, Dong et al.,²¹ showed that PANI-coupled graphitic carbon nitride

hybrids significantly improved the flame retardancy and waterproof properties of EP composites when combined with APP.

PANI has not been widely explored as a flame-retardant additive for polyolefins such as PE. However, there has been a few recent studies that investigated its flame retardancy in vinyl polymers such as polymethyl methacrylate and polystyrene. Zhan et al.,^{22,23} demonstrated the effectiveness of phosphorus-containing PANI as an electroconductive and flame-retardant additive for polymethyl methacrylate. Zhang et al.,²⁴ focused on PANI-montmorillonite nanocomposites modified with sodium dodecyl benzene sulphonate and 1,5-naphthalene disulfonic acid to enhance the flame retardancy of polystyrene. Their findings showed that these modifications significantly improved fire safety and thermal stability. In particular, the 1,5-naphthalene disulfonic acid-modified nanocomposite demonstrated the best flame retardancy performance due to its 3D network structure that reduced heat release and smoke production.

The studies reviewed showed that the choice of the doping acid had an effect on the flame retarding effect and electrical conductivity. APP is frequently used in IFR systems as an acid source and as a blowing agent.²⁵ APP could thus possibly make an effective IFR system for PE with PANI, with PANI functioning as a char precursor.⁷ There is also the possibility of APP and PANI combining synergistically as nitrogen based flame retardants are known to synergistically enhance the flame retardancy of phosphorus-based flame retardants.^{7,8} LDHs have previously been considered as flame retardants for PE.²⁶ Furthermore, Huang et al.²⁷ observed that wood impregnated with LDH-PANI nanofibrous aerogels had enhanced thermal insulation compared native wood.

Flame retardant, melt processible polymers with good mechanical properties are essential for various applications, including in the mining industry. The study aimed to assess the potential of PANI as a dual flame retardant and electrostatic dissipative additive for PE.

The objectives included synthesizing PE/PANI nanocomposites with 5 wt.% undoped PANI, PANI doped, and co-doped with various acids and PANI doped and modified with a double layered hydroxide (LDH) or APP. The nanocomposites were produced via in situ polymerization of aniline in the presence of polyethylene. Afterward, the nanocomposites were compression-molded into test specimens and their flame retardancy was evaluated using Underwriters Laboratory (UL) 94 tests and cone calorimetry. Structural and morphological was done through scanning electron microscopy (SEM) and Fourier-transform infrared spectroscopy (FTIR), while

thermal properties were assessed using differential scanning calorimetry (DSC) and thermogravimetric analysis (TGA). The study also evaluated the mechanical properties of the injection-molded PE/PANI nanocomposites using tensile tests. Additionally, the electrical conductivity of the nanocomposites was determined to assess their effectiveness for electrostatic dissipation applications.

2 | MATERIALS AND METHODOLOGY

2.1 | Materials

Analytical grade aniline, ammonium persulfate (APS), phosphoric acid (H_3PO_4), phytic acid, ammonia (NH_3), dodecylbenzenesulfonic acid (DBSA), magnesium chloride ($MgCl_2$), sodium dodecylbenzenesulfonate (SDBS), aluminium chloride ($AlCl_3$), and urea were purchased from Merck Life Sciences (Pty) Ltd. South Africa. Linear low-density PE was grade HR3950 (MFI 5 g/10 min at $190^\circ C/2.16$ kg) obtained from Sasol Polymers, South Africa, and APP (Exolit AP 766) was supplied by Clariant International Ltd. Turkey. All chemicals were used without further purification and all solutions were prepared with distilled water.

2.2 | Methods

PE/PANI nanocomposites with the compositions presented in Table 1 were prepared through in situ chemical oxidative polymerization of aniline in the presence of PE. The polymerization followed the scheme proposed by Stejskal et al.²⁸ The nanocomposites contained 5 wt.%

PANI. It was assumed that the formed PANI was completely protonated, with the PANI nitrogen atoms associated with counter anions from the acid dopant/co-dopant. In the co-doped PANI, equal amounts of each co-dopant were presumed. This allowed for calculating the repeat unit molecular weights of PANI-dopant and PANI-co-dopants, enabling the theoretical mass of PANI to be determined. Table 2 lists the reagents used in the polymerization.

2.2.1 | PE/PANI nanocomposites containing 5 wt. PANI doped with H_3PO_4 : PE/PANI(PPA)

The PE/PANI nanocomposites containing 5 wt.% PANI doped with H_3PO_4 were prepared by dissolving 15.5 mL (0.161 mol) of aniline in 1 M H_3PO_4 in a beaker to 150 mL by mixing with an electronic stirrer. A 45.005 g (0.201 mol) of APS was also dissolved in 1 M H_3PO_4 to 200 mL in a beaker by mixing with an electronic stirrer. Mixing was stopped in the APS solution when it became colorless. Two hundred and eighty five of PE powder were then added to the aniline solution and mixed vigorously until all the powder was fully immersed. The APS solution was then rapidly added to the aniline solution containing the immersed PE powder under vigorous mixing. The mixing was stopped when the mixture had turned blue; indicating the formation of the intermediate pernigraniline.²⁹ The mixture was subsequently immersed in an ice bath for 3 h to allow complete polymerization. The resulting PE/PANI(PPA) nanocomposite green precipitate was collected on a filter paper, vacuum filtered, and washed with three portions of 100 mL distilled water. To obtain the nanocomposite product in powder form, it was rinsed with acetone after washing

TABLE 1 PE/PANI nanocomposites formulations.

Formulations	Composition (wt.%)						
	PE	PANI (De-doped)	PANI (PPA) ^a	PANI (PPA/DBSA)	PANI (PPA/PA) ^b	PANI (PPA)-APP	PANI (PPA)-LDH
PE	100	95	95	95	95	90	90
PE/PANI(De-doped)	-	5	-	-	-	-	-
PE/PANI(PPA)	-	-	5	-	-	5	5
PE/PANI(PPA/DBSA)	-	-	-	5	-	-	-
PE/PANI(PPA/PA)	-	-	-	-	5	-	-
PE/PANI(PPA)-APP	-	-	-	-	-	5	-
PE/PANI(PPA)-LDH	-	-	-	-	-	-	5

Abbreviations: APS, ammonium persulfate; DBSA, dodecylbenzenesulfonic acid; LDH, double layered hydroxide; PANI, polyaniline; PE, polyethylene.

^aPPA: phosphoric acid.

^bPA: phytic acid.

TABLE 2 Amounts of reagents used in the in situ chemical oxidative polymerization of aniline in the presence of PE.

Formulations	PANI (wt.%)	PANI-Acid dopant/PANI-Acid co-dopant molecular wt. (mol/g)	Aniline (mL)	Aniline (mol)	APS (mol)	APS (g)	PANI (mol)	PANI (g)	PE	APP (g)	LDH (g)
PE	0	-	-	-	-	-	-	-	300	-	-
PE/PANI(De-doped)	5	344	-	-	-	-	-	15	285	-	-
PE/PANI(PPA) ^a	5	558	15.300	0.161	0.202	46.005	0.027	15	285	-	-
PE/PANI(PPA/DBSA)	5	786	15.297	0.161	0.202	54.995	0.019	15	285	-	-
PE/PANI(PPA/PA) ^b	5	1120	15.296	0.161	0.202	45.993	0.013	15	285	-	-
PE/PANI(PPA)-APP	5	558	15.300	0.161	0.202	46.005	0.027	15	285	15	-
PE/PANI(PPA)-LDH	5	558	15.300	0.161	0.202	46.005	0.027	15	285	-	15

Abbreviations: APS, ammonium persulfate; DBSA, dodecylbenzenesulfonic acid; LDH, double layered hydroxide; PANI, polyaniline; PE, polyethylene.

^aPPA: phosphoric acid.

^bPA: phytic acid.

with water.³⁰ The nanocomposite was then first air dried, and subsequently dried in an oven at 80°C for 12 h before further processing and analysis.

2.2.2 | PE/PANI nanocomposites containing 5 wt. PANI co-doped with either H₃PO₄ and DBSA: PE/PANI(PPA/DBSA) or H₃PO₄ and phytic acid: PE/PANI(PPA/PA)

The PE/PANI nanocomposites containing 5 wt.% PANI co-doped with either H₃PO₄ and DBSA that is, PE/PANI (PPA/DBSA) or H₃PO₄ and phytic acid that is, PE/PANI (PPA/PA) were prepared by dissolving 15.5 mL (0.161 mol) of aniline in an equimolar mixture of the relevant acids that is, either 1 M H₃PO₄ and 1 M DBSA or 1 M H₃PO₄ and 1 M phytic acid in a beaker to 150 mL. A 45.005 g (0.201 mol) of APS were also dissolved in the equimolar mixture of the relevant acids that is, either 1 M H₃PO₄ and 1 M DBSA or 1 M H₃PO₄ and 1 M phytic acid in a beaker to 200 mL in a beaker by mixing with an electronic stirrer. Two hundred and eighty five of PE powder were then added to the aniline solution and mixed vigorously until all the powder was fully immersed. In situ chemical oxidative polymerization of the aniline was then allowed to proceed as described in the section above.

2.2.3 | PE/PANI nanocomposites containing 5 wt. de-doped PANI: PE/PANI(De-doped)

The PE/PANI nanocomposite containing 5 wt.% PANI doped with H₃PO₄ was immersed in 5% NH₃ solution for 2 h. The PE/PANI nanocomposite powder changed from green to dark blue purple as soon as the NH₃ solution

was poured over the powder. The PE/PANI(De-doped) nanocomposite powder was subsequently collected on a filter paper, vacuum filtered and washed with three portions of 100 mL distilled water. It was then dried in air and subsequently in an oven for 12 h at 80°C.

2.2.4 | Synthesis and modification of the layered double hydroxide

The layered double hydroxide (LDH) used in this study was synthesized using the urea hydrolysis method.²⁶ An aqueous solution of Al³⁺ and Mg²⁺ with a molar fraction of Al³⁺/(Al³⁺ + Mg²⁺) equal to 0.33 was prepared by dissolving 2.225 g of AlCl₃ and 3.15 g of MgCl₂ in 100 mL distilled water. A 9.79 g of solid urea was added until the molar fraction urea/(Al³⁺ + Mg²⁺) reached 3.3. The solution was heated at 90–100°C for 36 h. The reaction was stopped by quenching in a water bath at room temperature after the reaction time had lapsed. The white LDH precipitate was then filtered, washed with distilled water and dried in an oven at 60°C for 12 h. Fifteen gram of the LDH was then dispersed in 25 mL of 0.15 M SDBS and stirred for about 24 h at 25°C. The modified solid was separated by repeated washing and centrifugation and subsequently dried at 60°C until the weight was constant.

2.2.5 | PE/PANI nanocomposites containing 5 wt. PANI doped with H₃PO₄ and modified with either the LDH: PE/PANI(PPA)-LDH or APP:PE/PANI(PPA)-APP

PE/PANI(PPA)-LDH and PE/PANI(PPA)-APP nanocomposites were prepared by dissolving 15.5 mL (0.161 mol)

of aniline in 1 M H_3PO_4 in a beaker to 150 mL by mixing with an electronic stirrer. A 45.005 g (0.201 mol) of APS was also dissolved in 1 M H_3PO_4 to 200 mL in a beaker by mixing with an electronic stirrer. Mixing was stopped in the APS solution when it became colorless. A 270 g of PE powder and 15 g of either APP or the LDH were then added to the aniline solution and mixed vigorously until all the powder was fully immersed. The APS solution was then rapidly added to the aniline solution containing the immersed PE powder and either the APP or the LDH under vigorous mixing. In situ chemical oxidative polymerization of the aniline was then allowed to proceed as described in the section above.

2.2.6 | Compression molding

PE/PANI nanocomposites sheets were compression molded using a heated press. The press was preheated to 160°C. The PE/PANI nanocomposite powder was then sandwiched in-between Teflon™ sheets inside a mold. The nanocomposites were pressed at 160°C and 15 MPa for 30 min. The molded sheets were then allowed to cool to room temperature at the same pressure of 15 MPa to prevent shrinkage. The molded sheets were subsequently cut into 100 × 100 × 3 mm³ specimens for cone calorimeter tests and 124 × 13 × 3 mm³ specimens for the Underwriters Laboratories UL-94 tests.

2.2.7 | Injection molding

Tensile tests specimens were injection molded using a TMC 30 (TMC Technology Corp., Taiwan, Republic of China). The parameters used for injection molding are given in Table 3.

2.3 | Characterization

The thermal stability of the neat PE and the PE/PANI nanocomposites was evaluated using TGA. The analysis was performed using a Perkin Elmer TGA 4000 instrument at a heating rate of 10°C/min from 40 to 800°C under nitrogen with a flow rate of 20 mL/min. Sample weight was maintained at 10 ± 0.5 mg.

The melting and crystallization behavior of the nanocomposites was studied through DSC using a Perkin Elmer DSC6000. The DSC thermograms were recorded from 40 to 220°C on second heating and cooling. The heating and cooling rate was kept constant at 10°C/min.

The functional groups on the nanocomposites were studied through Fourier transform infrared (FTIR)

TABLE 3 Injection molding parameters for tensile test specimens.

Parameter	Set Value
Temperature profile	180–200°C
Back pressure	10 bar
Injection pressure	95 bar
Cooling time	60 s
Mold temperature	25–35°C
Cycle time	160 s

spectroscopy. A Perkin-Elmer Spectrum 2 FTIR spectrometer with an attenuated total reflectance (ATR) accessory was used to record the IR spectra of the neat PE and the PE/PANI nanocomposites in the IR absorbance region of 3500–450 cm⁻¹, using 32 scans and a resolution of 4 cm⁻¹, for each sample.

A Zeiss high resolution scanning electron microscope equipped with an InLens detector was utilized to study the morphology of the nanocomposites, using an acceleration voltage of 5 kV and a working distance of 5 mm. The samples were sputtered with a thin layer of Au, prior to analysis. Elemental compositions of the nanocomposites were analyzed using an Oxford Aztec energy dispersive x-ray spectroscopy (EDX) detector coupled to the SEM.

The mechanical properties of the nanocomposites were evaluated through tensile tests using a Lloyds RX universal testing machine equipped with a 5 kN load cell. Testing was conducted at a crosshead speed of 50 mm/min, adhering to the ASTM D638-14 standard. The tests utilized injection-molded dumbbell-shaped specimens with a gauge length of 50 mm, a thickness of 3.75 mm and width of 10 mm. An average of three specimens was tested.

The flammability of the nanocomposites was studied through vertical burn tests and cone calorimetry. The vertical burning tests were conducted on a vertical burn instrument according to the UL 94:2001 standard. The dimensions of the specimens were 125 × 13 × 3 mm³. In this test, the specimens were clamped in a vertical position and ignited with a 20 mm blue flame held at a 45° angle, 10 cm away from the bottom end of the specimen. Cotton balls were placed 30 cm below the bottom of the specimen to catch any flaming particles that might drip from the test surface.

A Fire Testing Technology Dual Cone Calorimeter was used to conduct fire tests on the nanocomposites in accordance with the ISO 5660-1:2002 standard, using specimens with dimensions of 100 × 100 × 3.0 mm³. The rear of the specimen sheets was wrapped in aluminium foil, and the front of the specimens was exposed

horizontally to an external radiant heat flux of 35 kW/m². A retainer grid was placed on top of the samples to prevent them from expanding and touching the spark igniter. At least two tests were performed for each sample, with the average results reported.

A Major Tech MT1877 industrial multimeter was employed to measure the resistance R (Ω) of the nanocomposites. The volume resistivity of the nanocomposites (σ) was then determined using the Equation:

$$\sigma = RA/L, \quad (1)$$

where L (0.3 cm) was the distance between the two platinum probes and A (4.8 cm²) was the cross-sectional area of the samples. Two measurements were done for each sample and the average reported.

3 | RESULTS AND DISCUSSIONS

3.1 | Structural properties of the nanocomposites

3.1.1 | Fourier transform infrared spectroscopy

The FTIR spectra of the neat PE and the various PE/PANI nanocomposites prepared in the study are presented in Figure 1. The FTIR spectra in Figure 1 shows the characteristic IR absorption peaks exhibited by PE at wavenumbers 2916, 2848, and 1463–1472 cm⁻¹ which are ascribed to the C–H asymmetric stretching, symmetric stretching, and bending vibrations of –CH₂– groups, respectively. The peaks occurring in the IR region 719–730 cm⁻¹ are assigned to the distinctive C–C rocking vibration exhibited by long chains of methylene groups.³¹ The characteristic IR absorption peaks of PE identified above are also discernible in the IR spectra of the PE/PANI nanocomposites in Figure 1, with varying degrees of intensity.

FTIR was used to confirm the successful synthesis of the PANI in the present of the PE. Several of the characteristic IR adsorption bands exhibited by PANI were apparent in the FTIR spectra of the nanocomposites shown in Figure 1. The broad band centred at around 3250 cm⁻¹ was assigned to the H bonded N–H stretching. The IR broad bands between ca. 1360 and 1500 cm⁻¹ were ascribed to the benzenoid (N–B–N) structures in PANI (where B denotes the benzenoid moieties in the PANI chains), whereas the broad band between ca. 1500 and 1900 cm⁻¹ was assigned to the ring stretching of the quinoid (N=Q=N) structures in PANI, (where Q denotes quinoid moieties in the PANI chains).^{32,33} The emeraldine

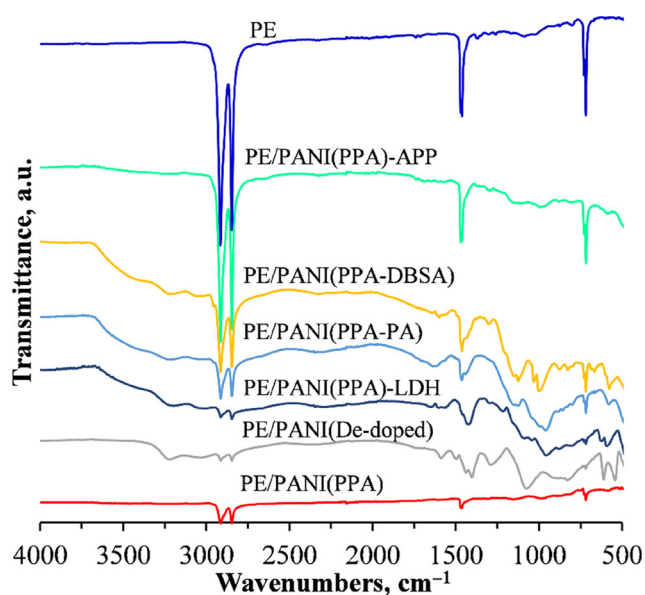


FIGURE 1 FTIR spectra of the neat PE, nanocomposites of PE and; PANI doped with H₃PO₄: PE/PANI(PPA); PANI doped with H₃PO₄ and modified with APP: PE/PANI(PPA)-APP; PANI doped with H₃PO₄ and modified with the LDH: PE/PANI(PPA)-LDH; PANI co-doped with H₃PO₄ and DBSA: PE/PANI(PPA)-DBSA; PANI co-doped with H₃PO₄ and phytic acid: PE/PANI(PPA)-PA; de-doped polyaniline: PE/PANI(De-doped). APP, ammonium polyphosphate; DBSA, dodecylbenzenesulfonic acid; FTIR, Fourier transform infrared; LDH, double layered hydroxide; PANI, polyaniline; PE, polyethylene.

base form of the PANI (the de-doped PANI) exhibited a sharper IR absorption band at ca. 1600 cm⁻¹, indicating the presence of the quinoid structures in this PANI form due to de-doping. The band at ca. 1200 cm⁻¹, was due to the C–N stretching of aromatic amines in PANI.³³ The bands around ca. 1000 cm⁻¹ were assigned to the vibrational modes of B–H⁺=Q or B–NH⁺–B. These bands result from the doping reactions of PANI and reflect the interaction between the PANI polymer chain and the dopants.^{34,35}

All the nanocomposites containing the doped PANI exhibited characteristic bands assigned to the phosphate counter ion, (PO₄)³⁻, around 500 cm⁻¹. This band is due to the deformation in the plane of the O–P–O bond.³⁶ In the spectrum of the PE/PANI nanocomposite with the PANI co-doped with phosphoric acid and DSBA, the characteristic IR absorption band of the sulfonic group (–SO₃H) was observed at ca. 1040 cm⁻¹.³⁷ Phytic acid shares its characteristic IR absorption band with phosphoric acid at around 500 cm⁻¹,³⁸ hence FTIR could not be used to independently confirm the presence of the counter ions derived from phytic acid, on the PANI structure of the nanocomposites co-doped with phosphoric acid and phytic acid, PE/PANI(PPA)-PA. The FTIR

results show that PANI was successfully synthesized in the presence of the PE.

3.1.2 | Scanning electron microscopy and energy dispersive x-ray analysis

Figure 2 shows the SEM micrographs of the neat PE and the PE/PANI nanocomposites at a magnification of 20,000 \times . Figure 2 shows a relatively smooth surface for the neat PE. The SEM results revealed that the PANI nanoparticles in the nanocomposite containing

PANI doped with phosphoric acid were agglomerated on the PE surfaces. The morphology of the PANI nanoparticles was not apparent, as the particles appeared to be covered by another material. It was inferred that this material covering the PANI nanoparticles might have been residual phosphoric acid, which was not completely washed off in the synthesis of the nanocomposites. However, in the micrograph of the nanocomposite containing de-doped PANI, the morphology of the nanoparticles was more discernible; they were composed of agglomerated, short nanosized rods. It is known that the morphology of the PANI nanoparticles

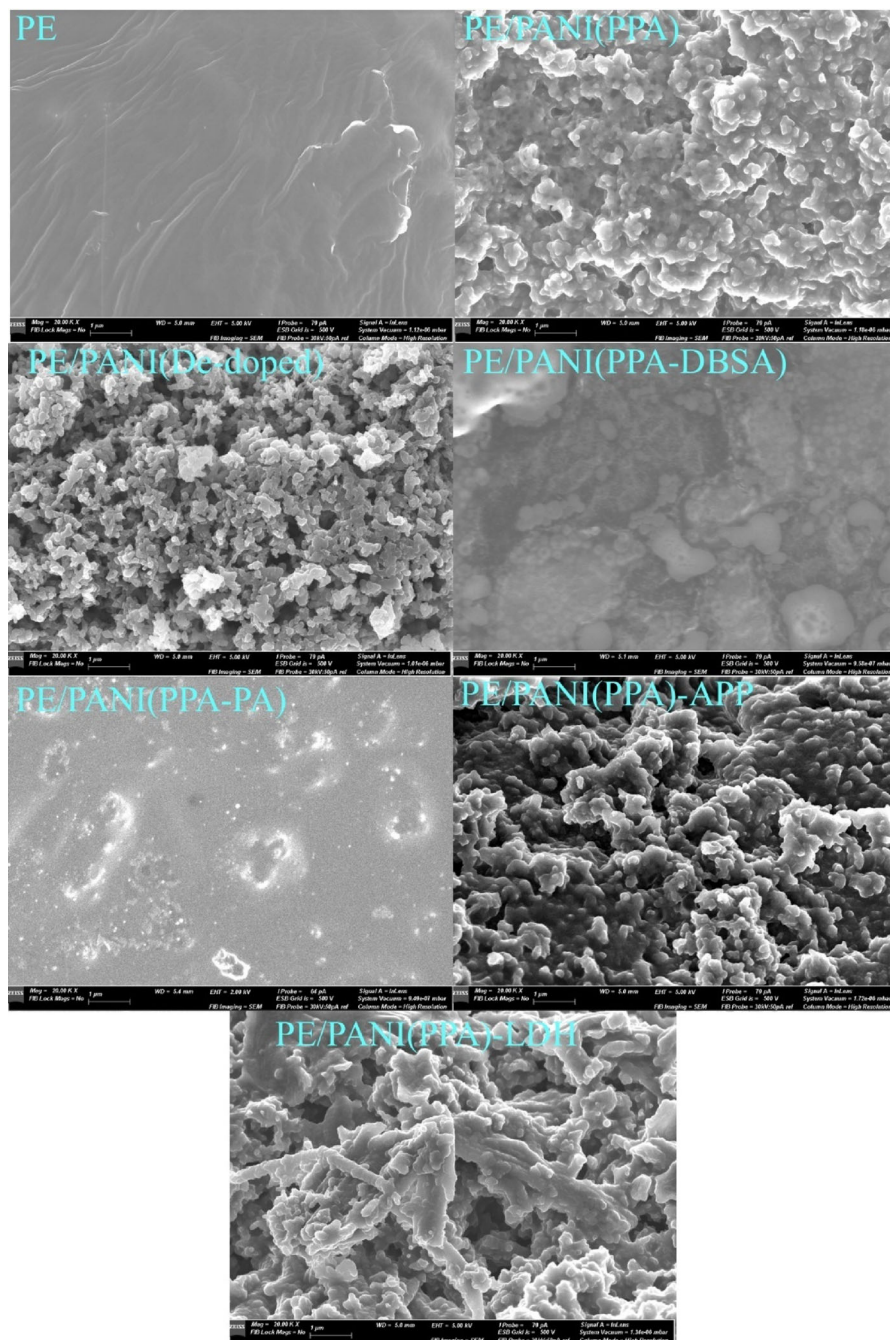


FIGURE 2 SEM micrographs of the neat PE, nanocomposites of PE and; PANI doped with H_3PO_4 : PE/PANI(PPA); PANI doped with H_3PO_4 and modified with APP: PE/PANI(PPA)-APP; PANI doped with H_3PO_4 and modified with the LDH: PE/PANI(PPA)-LDH; PANI co-doped with H_3PO_4 and DBSA: PE/PANI(PPA-DBSA); PANI co-doped with H_3PO_4 and phytic acid: PE/PANI(PPA-PA); de-doped polyaniline: PE/PANI(De-doped). APP, ammonium polyphosphate; DBSA, dodecylbenzenesulfonic acid; LDH, double layered hydroxide; PANI, polyaniline; PE, polyethylene; SEM, scanning electron microscopy.

depends on their preparation method and conditions, with agglomerated nanospheres typically obtained when chemical oxidative polymerization of aniline is conducted in strongly acid media.^{28,39}

In the nanocomposites of containing PANI co-doped with either phosphoric acid and phytic acid or with phosphoric and DBSA, the PANI nanoparticles were not apparent in the micrographs in Figure 2. This could again be attributed to the occurrence of residual acid on the PE surfaces after the synthesis of the PANI in the presence of the PE. The PANI nanoparticles in the nanocomposites containing PANI doped with phosphoric acid and modified with APP showed a similar morphology to those containing PANI doped with phosphoric acid, exhibiting a granular morphology agglomerated on the PE surfaces. However, the PANI nanoparticles in the nanocomposites containing PANI doped with phosphoric acid and modified with the LDH showed fibrillar morphology, although the nanofibres were also apparently coated on their surfaces. The fibrillar morphology is desirable in the synthesis of conductive PANI nanocomposites as high PANI aspect ratios enable the percolation threshold to be reached at lower PANI contents.

Table 4 shows the elemental compositions of the PE/PANI nanocomposites determined by EDX analysis. The EDX results in Table 4 exhibited significant variation, possibly due to inadequate dispersion being attained in the synthesis of the nanocomposites. The nanocomposite containing de-doped PANI was not expected to show the presence of the elements O, P, and S. However, the results in Table 4 show that these were present in this composite. The presence of O and P in this nanocomposite could have been due to incomplete de-doping of the phosphate counter ions or poor washing off of the residual H_3PO_4 used in the synthesis of nanocomposites. Stejskal et al.²⁸ previously showed that sulfuric acid

emanating from proton formation during the decomposition of the APS oxidant also participated in the protonation of the PANI, hence the presence of the S in all the nanocomposites. However, the EDX results in Table 4 show that all the nanocomposites contained significantly high levels of P and O, which could have been in the form phosphate counter ions attached to the PANI structure or residual H_3PO_4 .

The results in Table 4 also show that the nanocomposite, which contained PANI co-doped with phosphoric acid and DBSA had a relatively high content of S, due to the presence of the sulfonate counter ion as a dopant. The nanocomposite containing PANI doped with phosphoric acid and modified with the LDH also exhibited a relatively high content of S due to the use of SDBS in the synthesis and modification of the LDH. The EDX results in Table 4 also confirmed the presence of Mg and Al in the nanocomposites that had PANI doped with phosphoric acid and modified with the LDH.

3.2 | Thermal properties

3.2.1 | Differential scanning calorimetry

Figure 3 shows the DSC thermographs of the PE/PANI nanocomposites. Figure 3 shows that incorporating PANI into the nanocomposites did not significantly influence the melting and crystallization temperatures of the PE, no apparent changes were observed in the melting and crystallization temperatures.

3.2.2 | Thermogravimetric analysis

TGA was used to analyze the thermal stability of the PE/PANI nanocomposites. Figure 4 shows the TGA

TABLE 4 Elemental compositions of polyethylene (PE)/polyaniline (PANI) nanocomposites determined by EDX analysis.

Formulation	Element (at. %)						
	C	N	O	Mg	Al	P	S
PE/PANI(De-doped)	80 ± 10	4 ± 5	11 ± 3	-	-	3 ± 4	2 ± 3
PE/PANI(PPA) ^a	51 ± 24	7 ± 1	32 ± 13	-	-	8 ± 6	5 ± 4
PE/PANI(PPA/DBSA)	39 ± 8	6 ± 3	35 ± 5	-	-	7 ± 1	13 ± 2
PE/PANI(PPA/PA) ^b	40 ± 17	3 ± 2	36 ± 12	-	-	15 ± 7	7 ± 4
PE/PANI(PPA)-APP	49 ± 20	5 ± 4	33 ± 13	-	-	8 ± 6	5 ± 3
PE/PANI(PPA)-LDH	55 ± 21	5 ± 4	33 ± 12	0.22 ± 0	0.46 ± 0.21	10 ± 14	16 ± 27

Abbreviations: EDX, energy dispersive x-ray; DBSA, dodecylbenzenesulfonic acid; LDH, double layered hydroxide.

^aPPA: phosphoric acid.

^bPA: phytic acid.

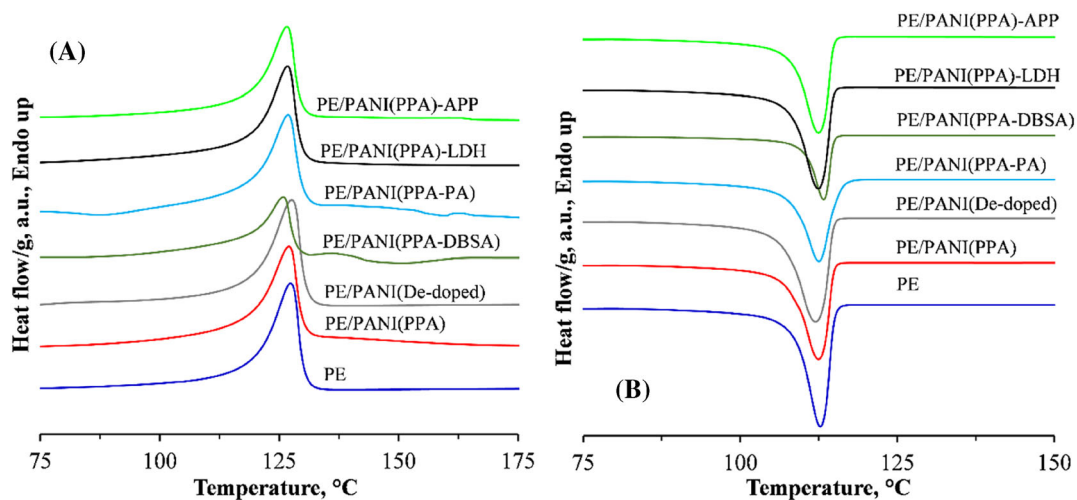


FIGURE 3 DSC thermographs of the neat PE, nanocomposites of PE and; PANI doped with H_3PO_4 : PE/PANI(PPA); PANI doped with H_3PO_4 and modified with APP: PE/PANI(PPA)-APP; PANI doped with H_3PO_4 and modified with the LDH: PE/PANI(PPA)-LDH; PANI co-doped with H_3PO_4 and DBSA: PE/PANI(PPA-DBSA); PANI co-doped with H_3PO_4 and phytic acid: PE/PANI(PPA-PA); de-doped polyaniline: PE/PANI(De-doped). APP, ammonium polyphosphate; DBSA, dodecylbenzenesulfonic acid; DSC, differential scanning calorimetry; LDH, double layered hydroxide; PANI, polyaniline; PE, polyethylene.

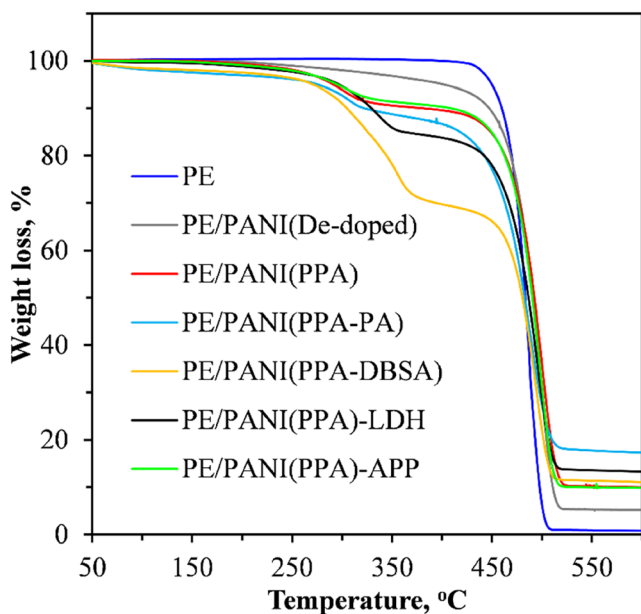


FIGURE 4 TGA curves of the neat PE, nanocomposites of PE and; PANI doped with H_3PO_4 : PE/PANI(PPA); PANI doped with H_3PO_4 and modified with APP: PE/PANI(PPA)-APP; PANI doped with H_3PO_4 and modified with the LDH: PE/PANI(PPA)-LDH; PANI co-doped with H_3PO_4 and DBSA: PE/PANI(PPA-DBSA); PANI co-doped with H_3PO_4 and phytic acid: PE/PANI(PPA-PA); de-doped polyaniline: PE/PANI(De-doped). APP, ammonium polyphosphate; DBSA, dodecylbenzenesulfonic acid; LDH, double layered hydroxide; PANI, polyaniline; PE, polyethylene; TGA, thermogravimetric analysis.

curves obtained for the neat PE and the PE/PANI nanocomposites. The TGA results showed that the neat PE had an onset degradation temperature of ca. $300^\circ C$. The

neat PE experienced a mass loss of almost 99% by the time it reached $500^\circ C$, producing a negligible char residue of only 1%. The nanocomposite containing de-doped PANI experienced a slight weight loss at about $100^\circ C$, attributed to the loss of moisture. Between ca. 150 and $400^\circ C$ this nanocomposite underwent a mass loss of about 5%, whereas the main degradation step occurred between ca. 400 and $500^\circ C$. It is interesting to note that the thermal degradation of this nanocomposite yielded a 5% residual mass (char), similar to the theoretical weight content of the PANI in the nanocomposite.

The nanocomposites, which contained PANI doped and co-doped with the various acids exhibited initial slight mass losses at temperatures below $150^\circ C$, due to moisture loss. At about $250^\circ C$, these nanocomposites experienced a second degradation step that is attributed to the degradation of the dopants. The nanocomposite, which contained PANI co-doped with phosphoric acid and DBSA exhibited the largest weight loss in this step of about 25%, whereas the nanocomposite that had PANI doped with phosphoric acid and modified with APP exhibited the least weight loss in this step of about 8%. The main degradation steps for these nanocomposites commenced at about $400^\circ C$, ending at around $425^\circ C$. Figure 4 also shows that all the nanocomposites synthesized with the doped PANI produced residual char yields of at least 10%, with the nanocomposite containing the PANI co-doped with phosphoric acid and phytic acid producing the largest amount of residual char upon thermal degradation (18%).

TABLE 5 UL 94 flammability tests data for the nanocomposites.

Formulations	UL-94 Rating	Ignition of cotton wadding	Total after-flame time (s)	Burning up to the clamp
PE	No rating	Yes	120 ± 7	Yes
PE/PANI(De-doped)	No rating	Yes	114 ± 7	Yes
PE/PANI(PPA) ^a	V2	Yes	55 ± 2	No
PE/PANI(PPA/DBSA)	V2	Yes	45 ± 5	No
PE/PANI(PPA/PA) ^b	V2	Yes	52 ± 7	No
PE/PANI(PPA)-APP	V2	Yes	56 ± 3	No
PE/PANI(PPA)-LDH	V2	Yes	54 ± 9	No

Abbreviations: APP, ammonium polyphosphate; DBSA, dodecylbenzenesulfonic acid; LDH, double layered hydroxide; PANI, polyaniline; PE, polyethylene.

^aPPA: phosphoric acid.

^bPA: phytic acid.

3.3 | Fire tests

3.3.1 | UL 94 flammability tests

Table 5 presents the UL 94 vertical flammability test results for the PE/PANI nanocomposites. In this test, the time during which the nanocomposites samples continued to burn after the ignition source was removed was recorded. Additionally, it was noted whether the nanocomposites dripped and ignited a wad of cotton placed below the sample holder.⁴⁰ During the tests, the neat PE burned violently and melted heavily. The melting that easily ignited the cotton wad. The neat PE could thus not be assigned a UL 94 rating, similar to prior studies.⁴¹ The nanocomposite containing de-doped PANI could also not be assigned a UL 94 rating. All its specimens burned up to the clamp, all specimens dripped and ignited the cotton wad. However, the results in Table 5 show that all the nanocomposites containing doped, co-doped, and modified PANI achieved a UL 94 V2 rating. These nanocomposites extinguished in less than half the time compared to neat PE and did not burn up to the clamp. This indicates that the doped, co-doped, and modified PANI imparted a flame-retardant effect to the PE.

The flammability of the PE/PANI nanocomposites was further investigated through cone calorimetry. Figure 5 and Table 6 show the typical HRR curves and a summary of the cone calorimeter data for the combustion of neat PE and PE/PANI nanocomposites. During the cone calorimeter tests, the neat PE samples melted progressively when exposed to the radiant heat flux, before volatilising and igniting. Some of the molten PE material flowed out of the aluminium foil containment. We previously reported similar challenges when testing the linear low density form of PE.⁴² Therefore, the data for the neat PE is questionable. For example, PE was expected to

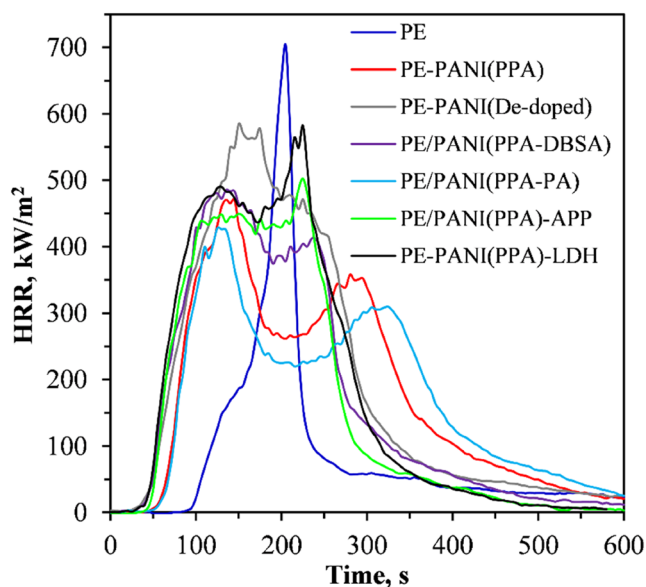


FIGURE 5 Heat release rate (HRR) curves of the neat PE, nanocomposites of PE and; PANI doped with H_3PO_4 : PE/PANI (PPA); PANI doped with H_3PO_4 and modified with APP: PE/PANI (PPA)-APP; PANI doped with H_3PO_4 and modified with the LDH: PE/PANI(PPA)-LDH; PANI co-doped with H_3PO_4 and DBSA: PE/PANI(PPA-DBSA); PANI co-doped with H_3PO_4 and phytic acid: PE/PANI(PPA-PA); de-doped polyaniline: PE/PANI(De-doped). APP, ammonium polyphosphate; DBSA, dodecylbenzenesulfonic acid; LDH, double layered hydroxide; PANI, polyaniline; PE, polyethylene.

exhibit a shorter ignition time (t_{ig}), and a higher pHRR. Hence, some of the cone calorimeter test results for PE such as the total heat released (tHR), and the maximum average rate of heat emission (MARHE) might have been negatively impacted by this observation. The tHR and MARHE results for the nanocomposites are also reported in Table 6.

TABLE 6 Cone calorimetry fire tests data of the PE/PANI nanocomposites showing the time to ignition (t_{ign}), time to flame out ($t_{\text{flame_out}}$), peak heat release rate (pHRR), time to peak heat release rate (t_{pHRR}), total heat released (tHR), maximum average rate of heat emission (MARHE), fire growth rate (FIGRA), Petrella fire growth index ($\text{pHRR}/t_{\text{ign}}$), and the fire performance index (FPI), and flame retardancy index (FRI).

Parameter	Units	Nanocomposite formulations						
		PE ^a	PE/PANI (PPA) ^b	PE/PANI (De-doped)	PE/PANI (PPA/DBSA)	PE/PANI (PPA/PA) ^c	PE/PANI (PPA)-APP	PE/PANI (PPA)-LDH
t_{ign}	s	69 ± 26	55 ± 7	30 ± 1	37 ± 4	51 ± 16	45 ± 6	28 ± 16
$t_{\text{flame_out}}$	s	1205 ± 172	634 ± 2	683 ± 171	660 ± 115	766 ± 10	524 ± 3	553 ± 102
pHRR	kW/m ²	571 ± 160	459 ± 17	614 ± 40	480 ± 8	392 ± 60	529 ± 38	575 ± 10
t_{pHRR}	s	173 ± 35	143 ± 4	150 ± 0	133 ± 4	115 ± 14	2.30 ± 7	225 ± 0
tHR	MJ/m ²	62.5 ± 9.3	103.3 ± 1.8	114.7 ± 3.4	100.8 ± 0.7	100.7 ± 1.4	96.7 ± 1.3	103.4 ± 6.0
MARHE	kW/m ²	161.6 ± 4.0	247.8 ± 6.1	353.7 ± 13	301.4 ± 12	200.7 ± 20	314.5 ± 0.3	346.4 ± 0.8
FIGRA	kW/m ²	3.28 ± 0.25	3.22 ± 0.04	4.09 ± 0.27	3.62 ± 0.03	3.41 ± 0.02	2.30 ± 7.1	2.56 ± 0.04
$\text{pHRR}/t_{\text{ign}}$	kW/m ² s	8.6 ± 0.9	8.4 ± 1.4	20.8 ± 0.9	13.1 ± 1.7	8.0 ± 1.6	11.9 ± 2.3	24.4 ± 13.9
FPI	m ² s/kW	0.119 ± 0.02	0.120 ± 0.02	0.048 ± 0.00	0.077 ± 0.01	0.127 ± 0.02	0.086 ± 0.02	0.049 ± 0.03
FRI	-	-	0.60	0.22	0.40	0.66	0.46	0.24

^aThe neat PE cone calorimeter results are suspect as the samples melted and dripped during the tests.

^bPPA: phosphoric acid.

^cPA: phytic acid.

Nevertheless, ignition resistance in the form of either higher piloted ignition temperatures or longer times to ignition (t_{ig}), and low pHRR are regarded as the key parameters to preventing fire growth. Ignition controls the flame spread and fire growth, whereas the pHRR controls the flame spread.⁴³ The results presented in Figure 5 and Table 6 show that the neat PE exhibited a relatively long t_{ig} of 69 s compared to the ignitions times of the PE/PANI nanocomposites which were less than 55 s, indicating that the nanocomposites exhibited lesser ignition resistance compared to the neat PE.

However, the neat PE had a significantly high pHRR, which reached up to 702 kW/m² (Figure 5), compared to the PE/PANI nanocomposites, signifying that combustion of the PE/PANI nanocomposites was less likely to result in fire growth and flame spread, compared to the neat PE. The results in Table 6 also show that co-doping of the PANI yielded the best flame retardancy effect with respect to the pHRR, similar to observations in other studies.^{8,13} The nanocomposite containing the PANI co-doped with phosphoric acid and phytic acid exhibited the best performance with the lowest pHRR of 392 kW/m² of all the nanocomposites, whereas the nanocomposite containing PANI doped with phosphoric acid had a pHRR of 459 kW/m².

It has been argued that the HRR is the single most important parameter in characterizing flammability and the attendant fire hazards posed by materials.^{44,45} In cone calorimetry, the HRR is determined by oxygen

consumption calorimetry.⁴⁵ The burning behavior of different types of materials can be elucidated from their HRR versus time curves.⁴⁵ The HRR curve for the neat PE shown in Figure 4 indicates that it is a thermally thin material, characterized by a sharp peak in its HRR. The shape of the HRR curve shows that the material is pyrolysed at the same time and does not form a char. This observation correlates with the TGA results in Figure 4.

The broad shape of the HRR curves of the nanocomposites presented in Figure 4 show that the nanocomposites where thermally thick charring (residue-forming)⁴⁵ materials in agreement with the TGA results presented and Figure 4. However, the HRR curves of the nanocomposites containing the doped and co-doped PANI exhibited two HRR peaks. The initial HRR peak is usually observed before charring, and the second peak occurs due to the produced char cracking or due to an increase in effective pyrolysis.⁴⁵ Therefore, the char formed through the combustion of the nanocomposites containing the doped PANI might not have been efficient at preventing further pyrolysis of the nanocomposites into gaseous fuel.

Table 5 further shows that all the PE/PANI nanocomposites exhibited shorter times to flame out compared to the neat PE, indicating that the PE sustained a flame for longer periods compared to the nanocomposites.

Several indices that are utilized to interpret cone calorimeter data in the assessment of the hazards posed due to fire developing from combustion of the materials being

tested are also presented in Table 6. The fire growth rate (FIGRA) estimates the rate of fire spread and the size of the fire.^{45,46} The FIGRA is defined as the maximum quotient of HRR(t)/t where HRR is the heat release rate as a function of time up to time t and divided by t . FIGRA is usually given by Equation (2) as:

$$\text{FIGRA} = \text{pHRR}/\text{time to pHRR}. \quad (2)$$

Lower FIGRA values indicate a decreased likelihood of material igniting and developing into a fire. Table 6 shows that the nanocomposites containing the PANI doped with phosphoric acid, PANI doped with phosphoric acid and modified with APP, and PANI doped with phosphoric acid and modified with the LDH, had lower FIGRA values compared to that of the neat PE. This indicates the effectiveness of the PANI in these particular formulations as a flame retardant for PE.

The fire growth index ($\text{pHRR}/t_{\text{ig}}$) proposed by Petrella⁴⁷ is an alternative estimator of the flame spread to FIGRA. Table 6 also shows that the nanocomposites containing PANI doped with phosphoric acid and the nanocomposites containing PANI co-doped with phosphoric acid and phytic acid had relatively lower fire growth indices compared to the neat PE. Thus, with respect to this fire growth index, which estimates the flame spread, the PANI doped with phosphoric acid and the PANI co-doped with phosphoric acid and phytic acid were the most effective flame retardants for PE.

Table 6 also shows the fire performance index (FPI) of the neat PE and the PE/PANI nanocomposites. The FPI is defined as the ratio of the time to ignition to the PHRR ($t_{\text{ig}}/\text{pHRR}$). A lower FPI indicates an accelerated flashover event, meaning materials with lower FPI values generally pose higher fire risks.⁴⁸ Table 6 shows that the nanocomposites that contained PANI doped with phosphoric acid and the nanocomposite that contained PANI co-doped with phosphoric acid and phytic acid had higher FPIs compared to the neat PE, whereas all the other nanocomposites had lower FPIs compared to the neat PE. Thus, with respect to the FPI, the nanocomposite that contained PANI co-doped with phosphoric acid and phytic acid was the most effective flame retardants for PE, followed by the nanocomposite that contained PANI doped with phosphoric acid.

The flame retardancy index (FRI) is a dimensionless index used to evaluate the flammability performance of polymers. Proposed by Vahabi et al.,⁴⁹ the FRI provides a quantitative assessment of the effectiveness of flame retardants in polymers. The FRI considers various factors such as the time to ignition, HRR, and total heat evolved during combustion. The FRI is determined as⁴⁹:

$$\text{Flame retardancy index (FRI)} = \frac{\left[\text{THR} \times \left(\frac{\text{pHRR}}{t_{\text{ig}}} \right) \right]_{\text{Neat Polymer}}}{\left[\text{THR} \times \left(\frac{\text{pHRR}}{t_{\text{ig}}} \right) \right]_{\text{Neat Polymer}}}, \quad (3)$$

where THR, pHRR, t_{ig} are the total heat released, PHRR and time to ignition respectively. According to the classification by Vahabi et al.,⁴⁹ composites with a FRI less than 1 ($\text{FRI} < 1$) exhibit poor flame retardancy characteristics. Composites with FRI values between 1 and 10 ($1 < \text{FRI} < 10$) indicate good flame retardancy performance, while FRI values ranging between 10 and 100 ($10 < \text{FRI} < 100$) suggest excellent flame retardancy.

The FRI values of the PANI nanocomposites synthesized in this study are presented in Table 6. According to the classification by Vahabi et al.,⁴⁹ all the nanocomposites synthesized in this study exhibited poor flame-retardant properties, with FRI values less than 1. This suggests that the PANI alone was insufficient as a flame retardant for PE or requires further modification to be enhance its flame-retardant properties.⁵⁰

The HRR curves for the PE/PANI nanocomposites in Figure 5 show that the nanocomposites formed a char during combustion, but it was not very coherent, contributing to their poor flame-retardant performance. However, nanocomposites where PANI was doped with phosphoric acid and PANI co-doped with phosphoric acid and phytic acid demonstrated relatively higher FRI values compared to the others. This indicates that these particular nanocomposites exhibited the best flame-retardant performance, consistent with the other results from the study.

Theoretically, PANI can function as a flame retardant in the vapor phase by thermally degrading into non-flammable gases such as CO_x , NO_x , H_2O , vaporized dopant molecules or degraded products and dopants. These can dilute the combustible gases from the matrix polymer. PANI could also enable the formation of a char that acts as a barrier to heat, oxygen and other pyrolysis products, thereby imparting flame retardancy through a condensed phase mechanism.^{6,7} The TGA results and HRR curves of the PE/PANI nanocomposites suggest that PANI doped with phosphoric acid and PANI co-doped with phosphoric acid and phytic acid are effective flame retardants for PE. This effectiveness is attributed to their ability to form a char during combustion, thus operating through a condensed phase mechanism. However, the double peaks observed in their HRR curves are evidence of the formed char not being a very effective barrier in blocking the heat from further pyrolysing the PE polymer into volatile fuel.

TABLE 7 Electrical polyethylene (PE)/polyaniline (PANI) nanocomposites.

Formulations	Resistivity (Ω cm)
PE	-
PE/PANI(De-doped)	-
PE/PANI(PPA) ^a	4.04×10^9
PE/PANI(PPA/DBSA)	3.02×10^9
PE/PANI(PPA/PA) ^b	4.00×10^8
PE/PANI(PPA)-APP	3.19×10^9
PE/PANI(PPA)-LDH	1.03×10^{-9}

Abbreviations: APP, ammonium polyphosphate; DBSA, dodecylbenzenesulfonic acid; LDH, double layered hydroxide.

^aPPA: phosphoric acid.

^bPA: phytic acid.

The improved flame retardancy performance of the PE/PANI nanocomposites containing PANI doped with phosphoric acid and also particularly the PANI co-doped with phosphoric acid and phytic acid could also have been due to the well-known phosphorus nitrogen flame retardancy synergy.^{7,8} Counter ions (phytate anions) emanating from phytic acid as a dopant contain more phosphorus atoms, compared to counter ions (phosphate anions) emanating from phosphoric acid.

3.4 | Volume resistivity

Electrical conductivity in PANI arises from the formation of polaron structures due to doping.⁷ The volume resistivity values of the PE/PANI nanocomposites synthesized in this study are presented in Table 7. The volume resistivities of the neat PE and the nanocomposite containing the de-doped PANI could not be determined, as their resistance was beyond the limits of the instrument used. However, the volume resistivity of polymers is known to range from 10^{15} to 10^{22} Ω cm, with PE at the higher end.⁴ The results in Table 7 show that the nanocomposite containing the PANI co-doped with phosphoric acid and phytic acid exhibited the lowest volume resistivity at 4×10^8 Ω cm. Nevertheless, the volume resistivity results in Table 7 show that all the PE/PANI nanocomposites synthesized with doped PANI exhibited volume resistivity values sufficiently low enough ($<10^{11}$ Ω cm) for fabricating electrostatic dissipative packing materials.^{51,52}

3.5 | Mechanical properties

The tensile mechanical properties of the PE/PANI nanocomposites are presented in Table 8. The results in

TABLE 8 Tensile mechanical properties of the polyethylene (PE)/polyaniline (PANI) nanocomposites.

Formulations	Tensile strength, MPa	Young's modulus, MPa	Elongation at break, %
PE	16.2 ± 0.5	195 ± 15	726 ± 113
PE/PANI(De-doped)	14.5 ± 0.7	208 ± 19	648 ± 223
PE/PANI(PPA) ^a	13.3 ± 0.1	151 ± 3	501 ± 264
PE/PANI(PPA/DBSA)	15.1 ± 0.1	214 ± 7	437 ± 72
PE/PANI(PPA/PA) ^b	15.1 ± 0.1	180 ± 8	557 ± 327
PE/PANI(PPA)-APP	12.8 ± 0.4	181 ± 41	662 ± 140
PE/PANI(PPA)-LDH	15.2 ± 0.0	181 ± 19	293 ± 0

Abbreviations: APP, ammonium polyphosphate; DBSA, dodecylbenzenesulfonic acid; LDH, double layered hydroxide.

^aPPA: phosphoric acid.

^bPA: phytic acid.

Table 8 indicate that all the PE/PANI nanocomposites exhibited reduced tensile strength compared to the neat PE. However, the reduction in tensile strength was limited to 9% for the best-performing PE/PANI nanocomposite in terms of flame retardancy, specifically the nanocomposite containing PANI doped with phosphoric acid and phytic acid.

The SEM results presented earlier showed that the PANI nanoparticles in the nanocomposites were agglomerated, indicating poor dispersion. This might have impacted on the tensile properties, particularly the tensile strength of the nanocomposites. As the PANI is stiffer than PE, it was expected that the PE/PANI nanocomposites would exhibit Young's moduli greater than that of the neat PE. However, only the PE nanocomposite containing the de-doped PANI and the nanocomposite containing PANI co-doped with phosphoric acid and DBSA exhibited Young's moduli values higher than that of the neat PE at 208 and 214 MPa, respectively. Again, this observation was attributed to poor dispersion of the PANI nanoparticles in the nanocomposites. The elongation at break results of the nanocomposites indicate that the PE/PANI nanocomposites retained useful ductility. For instance, the best-performing PE/PANI nanocomposite in terms of flame retardancy, the nanocomposite, which contained PANI doped with phosphoric acid and phytic acid, had an elongation to break of 557%, which was only 23% less than that of the neat PE.

4 | CONCLUSIONS

This study investigated the flame retardancy and electrical conductivity of PE nanocomposites reinforced with

polyaniline (PANI) doped, co-doped with various acids and modified with a layered double hydroxide (LDH) or with APP. The successful in situ synthesis of PANI in the presence of PE was confirmed through FTIR, while SEM revealed that the PANI formed short, nanosized rods. TGA demonstrated that the nanocomposites produced a char upon degradation, with the PANI co-doped with phosphoric acid and phytic acid yielding the highest char residue (~20%).

In flammability tests, all nanocomposites attained a V2 rating, and cone calorimeter data showed that incorporating the doped PANI into PE significantly reduced the pHRR. The nanocomposite with PANI co-doped with phosphoric and phytic acid exhibiting the lowest pHRR (392 kW/m²). However, the HRR curve indicated that the char formed was not effective enough to prevent further pyrolysis. This composite also had the lowest fire growth index and the highest FPI, demonstrating superior flame-retardant behavior. Although all the nanocomposites had FRI values less than 1, indicating overall poor flame retardancy performance, the PE/PANI nanocomposite with the PANI co-doped with phosphoric and phytic acid exhibited the highest FRI, confirming its relative flame retardancy.

Additionally, the volume resistivity of the nanocomposites (10⁸–10⁹ Ω·cm) suggested suitability for electrostatic dissipation (ESD) applications. Mechanically, the PE/PANI nanocomposites retained relatively good tensile properties with minimal deterioration due to PANI incorporation. In conclusion, the study highlighted PANI's potential as a flame-retardant additive for PE that also imparts electrostatic dissipation while preserving mechanical integrity. Further work is recommended to enhance the coherence and barrier properties of the char formed during combustion.

AUTHOR CONTRIBUTIONS

Conceptualization: Washington Mhike. **Methodology:** Washington Mhike, Vincent O. Ojijo, Joseph K.O. Asante, Vincent O. Ojijo, António B. Mapossa, Akeem Adisa. **Investigation:** Akeem Adisa. **Writing—original draft preparation:** Akeem Adisa. **Writing—review and editing:** Washington Mhike, Vincent O. Ojijo, Joseph K.O. Asante, Vincent O. Ojijo, António B. Mapossa. **Resources:** Washington Mhike, Vincent O. Ojijo, Joseph K. O. Asante. **Supervision:** Washington Mhike, Vincent O. Ojijo.

ACKNOWLEDGMENTS

The Council for Scientific and Industrial Research is acknowledged for availing their facilities and equipment.

FUNDING INFORMATION

The author(s) disclosed receipt of the following financial support for the research, authorship, and/or publication

of this article: A. Adisa received financial support under the Tshwane University of Technology (TUT) Postgraduate Scholarship. Authors received support from TUT for Open Accessing publishing.

CONFLICT OF INTEREST STATEMENT

The authors declare no conflicts of interest.

DATA AVAILABILITY STATEMENT

The datasets generated during and/or analyzed during the current study are available from the corresponding author on reasonable request.

ORCID

Washington Mhike  <https://orcid.org/0000-0003-4670-1171>

REFERENCES

- Luyt AS, Malik SS, Gasmi SA, et al. Halogen-free flame-retardant compounds. Thermal decomposition and flammability behavior for alternative polyethylene grades. *Polymers*. 2019;11:1479. doi:10.3390/polym11091479
- Zhou R, Mu J, Sun X, Ding Y, Jiang J. Application of intumescent flame retardant containing aluminum diethylphosphinate, neopentyl glycol, and melamine for polyethylene. *Saf Sci*. 2020;131:104849. doi:10.1016/j.ssci.2020.104849
- Jian L, Ning L, Yang S, Wang J, Hua M. Triboelectrification electrostatic potential of graphite/monomer casting nylon composites under dry sliding: correlation with electrical resistivity and wear mechanisms. *Polym Compos*. 2010;31:1369-1377. doi:10.1002/pc.20922
- Sun JS, Gokturk HS, Kalyon DM. Volume and surface resistivity of low-density polyethylene filled with stainless steel fibres. *J Mater Sci*. 1993;28:364-366. doi:10.1007/BF00357809
- Ai L, Yang L, Hu J, et al. Synergistic flame retardant effect of organic phosphorus–nitrogen and inorganic boron flame retardant on polyethylene. *Polym Eng Sci*. 2020;60:414-422. doi:10.1002/pen.25296
- Dasari A, Yu Z-Z, Cai G-P, Mai YW. Recent developments in the fire retardancy of polymeric materials. *Prog Polym Sci*. 2013;38:1357-1387. doi:10.1016/j.progpolymsci.2013.06.006
- Zarrintaj P, Yazdi MK, Vahabi H, Moghadam PN, Saeb MR. Towards advanced flame retardant organic coatings: expecting a new function from polyaniline. *Prog Org Coat*. 2019;130:144-148. doi:10.1016/j.porgcoat.2019.01.053
- Yu J, Zhou T, Pang Z, Wei Q. Flame retardancy and conductive properties of polyester fabrics coated with polyaniline. *Text Res J*. 2016;86:1171-1179. doi:10.1177/0040517515606360
- Bhadra S, Khastgir D, Singha NK, Lee JH. Progress in preparation, processing and applications of polyaniline. *Prog Polym Sci*. 2009;34:783-810. doi:10.1016/j.progpolymsci.2009.04.003
- Anand J, Palaniappan S, Sathyanarayana DN. Conducting polyaniline blends and composites. *Prog Polym Sci*. 1998;23:993-1018. doi:10.1016/S0079-6700(97)00040-3
- Terlemezyan L, Mokreva P. Electroactive polymer blends prepared in situ via bulk polymerization of aniline in the presence

- of polyethylene. *Int J Polym Mater*. 2002;51:23-30. doi:10.1080/00914030213032
12. Atanasov A, Koleva D. Electrically-conducting polyolefin composites containing disperse and fibre materials as conductive secondary phases. *Polym Polym Compos*. 2006;14:195-202. doi:10.1177/096739110601400
 13. Wu X, Qian X, An X. Flame retardancy of polyaniline-deposited paper composites prepared via in situ polymerization. *Carbohydr Polym*. 2013;92:435-440. doi:10.1016/j.carbpol.2012.09.032
 14. Bhat NV, Seshadri DT, Radhakrishnan S. Preparation, characterization, and performance of conductive fabrics: cotton + PANi. *Text Res J*. 2004;74:155-166. doi:10.1177/0040517504074002
 15. Stejskal J, Trchová M, Sapurina I. Flame-retardant effect of polyaniline coating deposited on cellulose fibers. *J Appl Polym Sci*. 2005;98:2347-2354. doi:10.1002/app.22144
 16. Salgaonkar LP, Jayaram RV. Thermal and flame-retardant properties of polyester fabric grafted with polyanilines. *J Appl Polym Sci*. 2004;93:1981-1988. doi:10.1002/app.20689
 17. Zhang X, He Q, Gu H, Colorado HA, Wei S, Guo Z. Flame-retardant electrical conductive Nanopolymers based on Bisphenol F epoxy resin reinforced with Nano polyanilines. *ACS Appl Mater Interfaces*. 2013;5:898-910. doi:10.1021/am302563w
 18. Mao H, Wu X, Qian X, An X. Conductivity and flame retardancy of polyaniline-deposited functional cellulosic paper doped with organic sulfonic acids. *Cellulose*. 2014;21:697-704. doi:10.1007/s10570-013-0122-1
 19. Zhong F, Chen C, Zhang D, et al. A novel dendritic polyaniline/phytate@Cu organic-metal composite flame retardant for improving thermal protection of epoxy coatings. *Colloids Surf A Physicochem Eng Asp*. 2023;670:131635. doi:10.1016/j.colsurfa.2023.131635
 20. Chen X, Piao J, Dong H, et al. Organic Phosphoric Acid Doped Polyaniline-Coupled g-C₃N₄ for Enhancing Fire Safety of Intumescent Flame-Retardant Epoxy Resin. *Macromol Rapid Commun*. 2023;44:2300071. doi:10.1002/marc.202300071
 21. Dong H, Wang Y, Feng T, et al. Phytic acid doped polyaniline-coupled g-C₃N₄ nanosheets for synergizing with APP promoting fire safety and waterproof performance of epoxy composites. *Polym Degrad Stab*. 2022;198:109879. doi:10.1016/j.polymdegradstab.2022.109879
 22. Zhan Z, Wang L, Zhang Y, et al. Fabrication of multifunctional polymethyl methacrylate composites based on phosphorus-containing polyaniline with excellent flame retardancy and electrical conductivity. *Polym Adv Technol*. 2021;32:1680-1689. doi:10.1002/pat.5205
 23. Zhan Z, Wang L, Duan R, et al. A novel strategy to improve the flame retardancy and electrical conductivity of polymethyl methacrylate by controlling the configuration of phosphorus-containing polyaniline@needle coke with magnetic field. *Chem Eng J*. 2022;448:137642. doi:10.1016/j.cej.2022.137642
 24. Zhang Z, Han Y, Li T, et al. Polyaniline/montmorillonite nanocomposites as an effective flame retardant and smoke suppressant for polystyrene. *Synth Met*. 2016;221:28-38. doi:10.1016/j.synthmet.2016.10.009
 25. Coimbra A, Sarazin J, Bourbigot S, Legros G, Consalvi JL. A semi-global reaction mechanism for the thermal decomposition of low-density polyethylene blended with ammonium polyphosphate and pentaerythritol. *Fire Saf J*. 2022;133:103649. doi:10.1016/j.firesaf.2022.103649
 26. Costa FR. *Mg-Al Layered Double Hydroxide: a Potential Nanofiller and Flame-Retardant for Polyethylene*. Technical University of Dresden; 2007.
 27. Huang H, Song SS, Shuai C-X, et al. Layered double hydroxide-Polyaniline nanofibers in lightweight aerogels for bioinspired flame-retardant wood. *ACS Appl Nano Mater*. 2023;6:4105-4111. doi:10.1021/acsnm.3c00195
 28. Stejskal J, Hlavatá D, Holler P, Trchová M, Prokeš J, Sapurina I. Polyaniline prepared in the presence of various acids: a conductivity study. *Polym Int*. 2004;53:294-300. doi:10.1002/pi.1406
 29. Stejskal J, Kratochvíl P, Jenkins AD. The formation of polyaniline and the nature of its structures. *Polymer*. 1996;37:367-369. doi:10.1016/0032-3861(96)81113-X
 30. Stejskal J, Gilbert RJP. Polyaniline. Preparation of a conducting polymer (IUPAC technical report). *Pure Appl Chem*. 2002;74:857-867. doi:10.1351/pac200274050857
 31. Alkan Ü, Kılıç M, Karabul Y, Yamak HB, Okutan M, İçelli O. Electrical and mechanical properties of LDPE/PANI composites. *J Nanoelectron Optoelectron*. 2016;11:343-348. doi:10.1166/jno.2016.1889
 32. Kang ET, Neoh KG, Tan KL. Polyaniline: a polymer with many interesting intrinsic redox states. *Prog Polym Sci*. 1998;23:277-324. doi:10.1016/S0079-6700(97)00030-0
 33. John A, Mahadeva SK, Kim J. The preparation, characterization and actuation behavior of polyaniline and cellulose blended electro-active paper. *Smart Mater Struct*. 2010;19:045011. doi:10.1088/0964-1726/19/4/045011
 34. Babazadeh MA. A direct one-pot method for synthesis of polyaniline doped with dodecyl benzene sulphonic acid in aqueous medium and study of its thermal properties. *Iran Polym J*. 2007;16:389-396.
 35. Benaouda SN, Chaker H, Abidallah F, et al. Heterogeneous photocatalytic degradation of anionic dye on polyaniline/microcrystalline cellulose composite. *J Porous Mater*. 2023;30:327-341. doi:10.1007/s10934-022-01342-x
 36. Campos PV, Albuquerque ARL, Angélica RS, Paz SPA. FTIR spectral signatures of amazon inorganic phosphates: igneous, weathering, and biogenetic origin. *Spectrochim Acta A Mol Biomol Spectrosc*. 2021;251:119476. doi:10.1016/j.saa.2021.119476
 37. Chen C-H, Wang J-M, Chen W-Y. Conductive Polyaniline doped with dodecyl benzene sulfonic acid: synthesis, characterization, and antistatic application. *Polymers*. 2020;12:2970. doi:10.3390/polym12122970
 38. Wang X, Zhang Y, Shi Y, Zeng X, Tang R, Wei L. Conducting polyaniline/poly(acrylic acid)/phytic acid multifunctional binders for Si anodes in lithium ion batteries. *Ionics*. 2019;25:5323-5331. doi:10.1007/s11581-019-03122-1
 39. Stejskal J, Sapurina I, Trchová M. Polyaniline nanostructures and the role of aniline oligomers in their formation. *Prog Polym Sci*. 2010;35:1420-1481. doi:10.1016/j.progpolymsci.2010.07.006
 40. Underwriters Laboratories. *UL Standard for Safety for Test for Flammability of Plastic Materials for Parts in Devices and Appliances, UL 94*. Underwriters laboratoris Inc.; 2021.
 41. Chen J, Wang J, Ni A, Chen H, Shen P. Synthesis of a novel phosphorous-nitrogen based charring agent and its application

- in flame-retardant HDPE/IFR composites. *Polymers*. 2019;11:1062. doi:10.3390/polym11061062
42. Mhike W, Ferreira IVW, Li J, Stoliarov SI, Focke WW. Flame retarding effect of graphite in rotationally molded polyethylene/graphite composites. *J Appl Polym Sci*. 2015;132:132. doi:10.1002/app.41472
43. Hull TR. 11—challenges in fire testing: reaction to fire tests and assessment of fire toxicity. In: Horrocks AR, Price D, eds. *Advances in Fire Retardant Materials*. Woodhead Publishing; 2008:255-290. doi:10.1533/9781845694701.2.255
44. Babrauskas V, Peacock RD. Heat release rate: the single most important variable in fire hazard. *Fire Saf J*. 1992;18:255-272. doi:10.1016/0379-7112(92)90019-9
45. Scharfel B, Hull TR. Development of fire-retarded materials—interpretation of cone calorimeter data. *Fire Mater*. 2007;31:327-354. doi:10.1002/fam.949
46. Sacristán M, Hull TR, Stec AA, Ronda JC, Galià M, Cádiz V. Cone calorimetry studies of fire retardant soybean-oil-based copolymers containing silicon or boron: comparison of additive and reactive approaches. *Polym Degrad Stab*. 2010;95:1269-1274. doi:10.1016/j.polyimdegradstab.2010.03.015
47. Petrella RV. The assessment of full-scale fire hazards from cone calorimeter data. *J Fire Sci*. 1994;12:14-43. doi:10.1177/073490419401200
48. Makhlof G, Hassan M, Nour M, Abdel-Monem YK, Abdelkhalik A. Evaluation of fire performance of linear low-density polyethylene containing novel intumescent flame retardant. *J Therm Anal Calorim*. 2017;130:1031-1041. doi:10.1007/s10973-017-6418-x
49. Vahabi H, Kandola BK, Saeb MR. Flame Retardancy index for thermoplastic. *Composites*. 2019;11:407. doi:10.3390/polym11030407
50. Vahabi H, Laoutid F, Movahedifar E, et al. Description of complementary actions of mineral and organic additives in thermoplastic polymer composites by flame retardancy index. *Polym Adv Technol*. 2019;30:2056-2066. doi:10.1002/pat.4638
51. ESD Association. ANSI/ESD S541-2019. Standard for Packaging ESD Susceptible Items. New York, USA 2019.
52. Electronic Industries Alliance. *JEDEC Standard: JESD625-A Requirements for Handling Electrostatic-Discharge-Sensitive (ESDS) Devices*. Electrostatic Discharge Association; 1999.

How to cite this article: Adisa A, Asante JKO, Ojijo VO, Mapossa AB, Mhike W. Polyaniline as a dual flame retardant and electrostatic dissipative additive in polyethylene nanocomposites. *J Vinyl Addit Technol*. 2024;1-17. doi:10.1002/vnl.22174